PAFR in adipose tissue macrophages is associated with anti-inflammatory phenotype and metabolic homeostasis

Luciano Ribeiro Filgueiras[1], Marianna Mainardi Koga[1], Paula G. Quaresma[3], Edson Kiyotaka Ishizuka[1], Marlise B. A. Montes[1], Patricia O. Prada[3,4], Mario J. Saad[3], Sonia Jancar[1],and Francisco J. Rios [2]

[1]Department of Immunology, Institute of Biomedical Sciences, University of Sao Paulo, Sao Paulo, Brazil
[2]Institute of Cardiovascular and Medical Sciences, British Heart Foundation Glasgow Cardiovascular Research Centre, University of Glasgow, Glasgow, United Kingdom
[3]Department of Internal Medicine, State University of Campinas (UNICAMP), Campinas, SP, Brazil
[4]School of Applied Sciences, State University of Campinas (UNICAMP), Limeira, SP, Brazil.

Corresponding author:
Francisco J. Rios, PhD
Institute of Cardiovascular & Medical Sciences
BHF Glasgow Cardiovascular Research Centre
University of Glasgow
126 University Place
Glasgow
G12 8TA
Tel: + 44 (0) 0141 330 8015
Fax: + 44 (0)141 330-3360
Email: Francisco.Rios@glasgow.ac.uk

Abstract

Metabolic dysfunction is associated with adipose tissue inflammation and macrophage infiltration. The Platelet Activating Factor Receptor (PAFR) is expressed in several cell types and binds to PAF and oxidized phospholipids. Engagement of PAFR in macrophages drives them towards the anti-inflammatory phenotype. In the present study, we investigated whether genetic deficiency of PAFR affects the phenotype of adipose tissue macrophages (ATM) and its effect on glucose and insulin metabolism. PAFR-deficient (PAFRKO) and wild type mice (WT) were fed standard (SD) or high fat diet (HFD). Glucose and insulin tolerance tests were performed by blood monitoring. ATM were evaluated by FACS for phenotypic markers. Gene and protein expression was investigated by real-time PCR and western-blot, respectively. Results showed that the epididymal adipose tissue of PAFRKO mice had increased gene expression of *Ccr7, Nos2, Il6, and Il12,* associated topro-inflammatory mediators, and reduced expression of the anti-inflammatory *IL10*. Moreover, the adipose tissue of PAFRKO presented higher pro-inflammatory macrophages, characterized by an increased frequency of $F4/80^{+}CD11c^{+}$ cells. Blood monocytes of PAFRKO mice also exhibited a pro-inflammatory phenotype (increased frequency of Lys6C+.cells) and PAFR-ligands were detected in the serum of both PAFRKO and WT. Regarding metabolic parameters, compared to WT, PAFRKO mice had: i) higher weight gain andserum glucose concentration levels; ii) decreased insulin-stimulated glucose disappearance; iii) insulin resistance in the liver; iv) increased expression of Ldlr in the liver. In mice fed HFD, some of these changes were potentiated, particularly in the liver. Thus, it seems that endogenous ligands of PAFR are responsible for maintaining the anti-inflammatory profile of blood monocytes and adipose tissue macrophages under physiological conditions. In the absence of PAFR signaling, monocytes and macrophages acquire pro-inflammatory phenotype, resulting in adipose tissue inflammation and metabolic dysfunction.

Summary
We found an essential role of PAFR in adipose tissue macrophages. The PAFR-deficiency leads to infiltration of pro-inflammatory macrophages in the adipose tissue resulting in weight gain, reduced glucose tolerance, hepatic insulin resistance, followed by hepatic steatosis.

Short Title: PAFR is associated with anti-inflammatory macrophages and glucose metabolism

Keywords: Macrophages, adipose tissue, platelet-activating factor receptor, glucose, insulin.

Introduction

The incidence of insulin resistance, the hallmark of Type 2 Diabetes (T2D), has increased dramatically as a consequence of the increase in worldwide obesity (1, 2). Under physiological conditions, the adipose tissue contributes to homeostasis by producing hormones, lipid mediators, adipokines, and growth factors, which play an important role in glucose metabolism. In the obese stage, however, adipose tissue shows a high inflammatory profile that leads to metabolic disturbances such as glucose intolerance and insulin resistance (3).

Adipose tissue macrophages (ATM) are the predominant leukocyte observed in metabolically healthy and also insulin-resistant fat in both humans and mice models (4, 5). In metabolically healthy conditions, ATM represent between 5-10% of the total cell population in white adipose tissue (WAT) and exhibits an anti-inflammatory or M2 profile, whereas obesity is accompanied by increased ATM infiltration, presenting a pro-inflammatory M1 profile (6, 7).

Monocyte recruitment to adipose tissue during obesity is an important step in the development of insulin resistance. Deficiency of the chemoattractant Ccr2 or its receptor blunts monocyte mobilization to the fat and protects mice from diet-induced insulin resistance, although they still present obesity (8). Similar results were found in mice depleted of macrophages (9) or that lack the receptor for the lipid mediator leukotriene B4, BLT-1 (10). The shift to classically activated or pro-inflammatory M1 macrophages in the adipose tissue is correlated with the production of cytokines such as interleukin (IL)-6, IL-1β, and Tumor Necrosis Factor (TNF)-α and insulin resistance (5). ATMs are also efficient antigen-presenting cells that are able to induce effector/memory $CD4^+$ T cell proliferation (Th1) in visceral fat, potentiating adipose tissue inflammation (11).

Platelet activating factor (PAF) is a lipid mediator secreted by many cell types through enzymatic hydrolysis catalyzed by phospholipase A2, which acts at nanomolar concentration (12). The PAF receptor (PAFR) is a G-protein coupled receptor expressed in plasma and nuclear membranes of many cell types, including macrophages, that binds not only to PAF but also to a wide range of non-enzymatically generated oxidized phospholipids (13). We have previously shown that apoptotic cells and oxidized low density lipoproteins express moieties that bind to PAFR and are cleared by macrophages through the scavenger receptor CD36 in association with PAFR (14, 15). We also found that this process induces functional changes in macrophages, compatible with the regulatory phenotype or M2 proposed by Mosser and Edwards (16), with the secretion of anti-inflammatory mediators/cytokines.

Recently, Yamaguchi et al. demonstrated that the knock down of PAFR in mice results in increased adiposity and increased susceptibility to diet-induced obesity (17). Overall, their results suggest that the anti-obesity effect of PAFR is due to impaired energy expenditure. Regarding WAT inflammation, they found that the CD11c+ macrophage (M1) population was increased in PAFR-deficient mice, although they did not find any increased levels of pro-inflammatory markers (17, 18). Contrarily, Menezes-Garcia et al. found that PAFR deficiency resulted in decreased inflammation in the adipose tissue and improved glucose metabolism (19). In a complex system involving the systemic and adipose tissue inflammation and metabolic dysfunction, the mouse strain, the diet composition, and even gender matters. For example, high fat diet increased adiposity in both male and female rats but, whereas the male developed insulin resistance, the female maintained insulin sensitivity (20). Meneses-Garcia et al. used male C57Bl/6 and high-refined carbohydrate-containing diet whereas Yamagushi et al, used C57Bl/6 and hight fat diet (60% fat)(17, 19). Balb/c also differ from C57Bl/6

mice in the response to PAF, since Balb/c mice are more resistant to shock induced by intravenous injection of PAF (21).

In the present study we investigate the role of PAFR and adipose tissue macrophages in regulate metabolic homeostasis by comparing PAFR knockout (PAFRKO) and wild type (WT) mice of Balb/c background, fed by standard or high fat diet (HFD).

Methods

Animals

BALB/c mice WT and PAFRKO animals, 8 to 10 weeks old (young adult), were housed in a specific pathogen-free facility in a room with a 12 h light–dark cycle with water and food *ad libitum*. Animal care and research protocols were in accordance with the principles and guidelines adopted by the Brazilian College of Animal Experimentation (COBEA) and this project was approved by the Ethical Committee for Animal Research of the Institute of Biomedical Sciences of the University of São Paulo. A group of mice receiving a standard rodent chow were compared with a group that received a high-fat diet with 55% calories from fat for 12 consecutive weeks, as previously described (22). Body weight was recorded weekly. Glucose and insulin tolerance tests were performed on the 12th week of feeding in high fat diet. A group of WT and PAFRKO mice was kept on standard diet for 40 weeks (aged mice). PAFRKO mice were originally obtained from Drs. Satoshi Ishii and Takao Shimizu (23).

Glucose/insulin tolerance tests

After 6 h fasting, mice were anesthetized by an i.p. injection of sodium amobarbital (15 mg/kg body weight), and the experiments were initiated after the loss of corneal and pedal reflexes. The glucose tolerance test (GTT) was conducted by i.p. injection of a 20% glucose solution (2 g/kg body weight). The insulin tolerance test (ITT) was performed by i.p. injection of insulin (1.5 U/Kg). Blood samples were collected from the tail vein at 0, 30, 60, 90, and 120 min and the glucose concentrations were assessed using a glucose monitor (Glucometer, Bayer).

Tissue extraction and immunoblotting

Mice were anesthetized by intraperitoneal injection of a Ketamine/Xylazine cocktail. Five minutes after the insulin injection (3.8 U/kg i.p.), the liver, muscle, and adipose tissue were removed, minced coarsely, and homogenized immediately in extraction buffer, as described elsewhere. Protein concentrations were determined by the BCA kit (Thermo Scientific, Rockford, IL, USA). Equal amounts of proteins were separated by 10% SDS-PAGE and transferred to a Hybond™ nitrocellulose membrane (GE Healthcare, NJ, USA). The non-specific binding was blocked with non-fat dry milk. Membranes were incubated overnight at 4ºC and under constant stirring with primary antibodies specific for phosphorylated or total form of Akt (Cell Signaling Technology, Beverly, MA, USA). As secondary antibodies, we used anti-rabbit IgG-HPR (Cell Signaling Technology, Beverly, MA, USA). Expression was visualized using SuperSignal West Pico Chemiluminescent Substrate (Thermo Scientific, Rockford, IL, USA).

Histology

Epididymal adipose tissue and liver were fixed in a 10% buffered-formalin solution and routinely processed for histological inclusion in paraffin. Five-µm thick tissue sections

were stained with Hematoxylin and Eosin (HE) and observed in a light microscope. The adipocyte area was determined using the package ImageJ 1.44p (Wayne Rasband, NIH, USA) available in http://imagej.nih.gov/ij.

Peripheral Blood Mononuclear Cells (PBMCs) preparation and FACS analysis
Whole blood samples were collected from mice and PBMCs were isolated by Ficoll-Paque PLUS (GE Healthcare) density gradient centrifugation according to manufacturer's instructions. Isolated cells were extensively washed with ice cold PBS and stained for flow cytometry analysis. Cell pellets were re-suspended in FACS buffer (PBS 0,1% sodium azide, 1% FBS) and stained with fluorescent-conjugated monoclonal antibodies anti-Ly6C-PE (HK1.4) (eBioscience, San Diego, CA, USA) and anti-CD11b-FITC (M1/70) (BD Pharmingen, Franklin Lakes, NJ, USA). After extensive washing, stained cells were analyzed using a FACSCanto II flow cytometer (BD Biosciences). Results were collected at 100,000 cells and analyzed using FlowJo software (TreeStar, Ashland, USA). Ly6C+ populations were determined on CD11b+ gated cells.

Determination of ATM phenotype by FACS
Epididymal adipose tissue was digested in PBS with collagenase IV (1 mg/mL) (Sigma-Aldrich, St Louis, MO, USA) in constant agitation at 37ºC for 30 min. The final cell suspension was centrifuged at 300 x g and washed twice with ice cold PBS and stained for flow cytometry analysis. Cell pellets were re-suspended in FACS buffer (PBS with 2% FBS) and stained with fluorescent-conjugated monoclonal Antibodies anti-F4/80-PE, anti-CD11c-APC, and anti-CD206-FITC (BD Biosciences, Franklin Lakes, NJ, USA). After extensive washing, stained cells were analyzed using a FACSCanto II flow cytometer (BD Biosciences). Results were collected at 30,000 cells and analyzed using FlowJo software (TreeStar, Ashland, USA).

Culture of Macrophages
Peritoneal exudate cells were obtained by lavage of the peritoneal cavity with cold PBS. The fluid lavage was centrifuged (400 ×g, 10 min, 4°C). The cellular concentration was adjusted to 2×10^6 cells/mL with RPMI 1640 medium, supplemented with 10% FCS, streptomycin (100 µg/mL), penicillin (60 U/mL), sodium bicarbonate (11 mM), l-glutamine (2 mM), and HEPES (20 mM). Cells were left to adhere on microplates for 2 h at 37°C in a 5% CO_2. Non-adherent cells were removed by aspiration of the supernatant and replacement with fresh medium RPMI/2% FBS overnight before experiments.

mRNA expression
RNA was isolated using TRIzol reagents (Life Technologies, Carlsbad, CA, USA). For the real-time reverse-transcriptase polymerase chain reaction (PCR), cDNA was synthesized using the RevertAid^{TM} First Strand cDNA Synthesis Kit (Fermentas Life Sciences, Ontario, USA), according to the manufacturer's instructions. PCR-master mix (Power SyBr® Green, Applied Biosystems, Warrington, UK) containing the specific mouse primers, as fallow: IL-6, IL-12, IL-10, iNOS, CCR7, Chemerin, and Adiponectin (Supp Table S1)). Relative gene expression was calculated by the $2^{-\text{Delta Delta C(T)}}$ method, as previously described (24). Data are shown as the fold-change in expression of the target gene relative to the internal control gene (GAPDH).

PAFR-ligands in the serum

The presence of systemic PAFR-ligands in lipid extracted from serum of PAFR KO and WT mice was determined as their ability to induce IL-8 production in human keratinocytes transfected with PAFR (KBP cells), but not in keratinocytes lacking the PAFR (KBM cells) as previously described (25). Briefly, 2 x 10-5 KBM and KBP cells were plated in 12 wells plates and cultures overnight in Dulbecco´s modified Eagle´s medium (DMEM) containing 10% of fetal bovine serum (FBS). The cells were then washed with PBS, and DMEN without FBS was added. The cells were stimulated with lipid extract from PAFR KO and WT mice serum and after 6 hours the supernatants were collected for IL-8 measuremen by ELISA. The concentration of IL-8 induced by the lipids extracts was compared to that induced by a stable PAF-R agonist 1-hexadecyl-2-N-methylcarbamoyl glycerophosphocholine (cPAF).

Cytokine Measurement and Biochemical analyses

IL-10, IL-1β and IL-8 concentration in the supernatants of macrophages were measured using BD OptEIA^{TM}ELISA Set (BD Biosciences, San Diego, CA, USA). For biochemical analysis, plasma from PAFRKO and WT mice were harvested and the concentration of alanine aminotransferase (ALT), aspartate aminotransferase (AST) and lactate dehydrogenase (LDH) were determined by colorimetric assay using commercially available kits (Bioclin, Belo Horizonte, MG, Brazil) according to the manufacturer's instructions.

Statistical analysis

Data are presented as mean ± SEM. Analysis of variance (ANOVA) and the Student-Newman-Keuls post-test were used to evaluate the statistical significance of the differences between three or more groups. Two-tailed unpaired Student's t-test was used when differences between two groups were analyzed. Significance was assumed if $p < 0.05$.

Results

PAFR deficiency is associated with pro-inflammatory phenotype of adipose tissue macrophages and blood monocytes.

Since the homeostasis of WAT is dependent on the activation phenotype of the adipose tissue macrophages (26, 27), epididymal adipose tissue was processed and the final cell suspension was submitted to FACS analysis for total macrophages ($F4/80^+$ cells), pro-inflammatory M1 ($F4/80^+$ $CD11c^+$) and anti-inflammatory M2 macrophages ($F4/80^+CD206^+$). In PAFRKO mice, the macrophage F4/80+ population in WAT, as well as the M1 and M2, were increased when compared to the WT (Fig 1A-C). The M1 population was increased 2-fold in PAFRKO mice. Adipose tissue from PAFRKO mice presented increased gene expression of the M1 macrophages markers IL-12, IL-6, iNOS and CCR7 (Fig 2A-D) and lower levels of the M2 marker IL-10 (Fig 2E). The pro-inflammatory phenotype in PAFRKO macrophages was confirmed by the IL12/IL10 ratio which was 0.87 in the PAFRKO and 0.17 in the WT (Fig 2F). Next, we investigated adipokines in the WAT of PAFRKO and WT and similar levels of the pro-inflammatory chemerin and anti-inflammatory adiponectin were found (Fig 2G and 2H).

Peritoneal resident macrophages from PAFR KO mice also presented pro-inflammatory phenotype. Following LPS stimulation, macrophages from PAFR KO mice produced increased amounts of IL-1β, reduced levels of IL-10 (Supp. Fig1A-B), and increased gene expression of M1 markers IL-6, IL-12 and iNOS (Supp. Fig S1C and S1D).

Aging and HFD had similar effects on ATM. Fig 3A shows that 40 week-old PAFRKO mice presented higher $CD11c^+$ population, while no difference was found in the $CD206^+$ population and the same was observed in mice (8-10 weeks old) fed the HFD (Fig 3B).

In the blood, $CD11b^+Ly6C^{int}$and $CD11b^+Ly6C^{high}$ mononuclear cells are considered to be pro-inflammatory monocytes that are bound to differentiate into M1 inflammatory macrophages (28). Although no difference in $CD11b^+$ $Ly66C^{int}$ population was found between PAFR KO and WT mice, PAFR KO mice presented a significant increased population (3 times higher) of $Ly6C^{high}$ of $CD11b^+$ cells, indicating that the lack of PAFR promotes an increase in the pro-inflammatory monocytes population (Fig 4A and 4B).

Because PAFR can be engaged by a wide range of oxidized lipids, we measured the total PAFR binding activity in the blood using the semi-quantitative assay described in Methods. This was done using a human keratinocytes cell line transfected with PAF-receptor (KBP cells) that produce IL-8 when the receptor is activated (25). We then exposed the PAF-receptor expressing cells (KBP) or the PAF-receptor negative (KBM) cells for 6 h to total lipids extracted from the serum of PAFR-KO and WT mice and measured IL8 concentration in the supernantants. The concentration of IL-8 induced by the lipid extracts was compared to the IL-8 induced by the metabolically stable PAF-R agonist 1-hexadecyl-2-*N*-methylcarbamoyl glycerophosphocholine (cPAF).It was found that the serum of both, WT and PAFR KO presented PAFR activity, equivalent to the activity of 14 -15 nM of cPAF.

Together, these results indicate that PAFR ligands present in the serum of PAFR KO and WT mice, engage PAFR in monocytes/macrophages promoting anti-inflammatory phenotype.

PAFR deficiency is associated with reduced glucose and insulin tolerance

When fed the SD, the PAFRKO and WT mice have similar body weight gain over 12 weeks. When fed a HFD, the PAFRKO mice showed a significantly higher weight gain than the WT group (Fig 5A). Increased adipocyte size is indicative of obesity and we found that the adipocytes in the HFD group were significantly larger than in those fed the SD, which was observed in both PAFRKO and WT mice (Fig 5B). PAFRKO mice showed increased epididymal fat and liver weight (Fig 5C and 5D). These results indicate that PAFRKO mice are more susceptible to develop metabolic syndrome.

Figure 6A shows that PAFRKO mice develop evident hepatosteatosis, a hallmark of metabolic syndrome, when fed HFD. PAFRKO mice fed SD already present disarrangement of hepatocytes. We then analyzed the liver of mice fed a SD for expression of two lipogenic genes (Ldlr and Srebf1). Figure 6B shows that the PAFRKO express higher levels of LdlrmRNA, but no significant differences were found in Srebf1 expression (Fig 6C). Biochemical markers of liver damage (AST, ALT, and LDH) were also determined in the plasma and no difference was found comparing PAFRKO and WT mice under SD (Fig 6D and 6F). These results suggest that under SD the PAFRKO mice although already express increased level of the lipogenic gene Ldlr and hepatocytes dissarangement, but only when fed HFD they develop liver steatosis.

We then investigated whether PAFR deficiency was associated with imbalanced glucose metabolism. Measuring the fasting glycemia, we found that PAFRKO fed the SD already presented higher serum glucose levels than the WT. HFD increased glucose levels in both WT and PAFRKO (Fig 7A). To evaluate whether the higher levels of glucose found in PAFRKO mice were associated with insulin resistance, we performed

Glucose and Insulin Tolerance Tests (GTT and ITT). PAFRKO mice were shown to be more glucose intolerant than WT in both SD and HFD (Fig 7B and 7C). Importantly, PAFRKO mice fed with SD were already insulin resistant, suggesting a central role for PAFR in glucose metabolism (Fig 7D). In HFD, PAFRKO mice also presented a more prominent insulin resistance than the control group (Fig 7E).

Deficiency of PAFR reduces insulin signaling

We next investigated the insulin-induced AKT phosphorylation in two different insulin target organs. In the liver, the absence of PAFR was sufficient to promote insulin resistance, since PAFRKO mice fed SD already presented insulin-signaling impairment, an effect that was maximized in mice fed the HFD (Fig 8A). In the skeletal muscle, which is the second organ to develop diet-induced insulin resistance (29), we found that the HFD induced insulin resistance only in the PAFR-deficient mice. Moreover, the insulin signaling was preserved in WT animals fed with HFD (Fig 8B). These results suggest that the deficiency of PAFR promotes susceptibility to insulin resistance.

Discussion

In the present study, we found an essential modulatory role of PAFR in blood monocytes and adipose tissue macrophages. In PAFRKO mice, an increased population of activated monocyte ($Ly6C^{high}$ $CD11b^{+}$) cells in the blood and increased number of $F4/80^{+}$ macrophages expressing the M1 marker CD11c in the epididymal fat tissuewas found. The adipose tissue presented higher mRNA levels of some M1 markers, increased IL-12 and reduced IL-10 levels. The balance of IL-12 and IL-10 had been previously employed to establish the macrophages phenotype: the classically activated or M1 macrophages and the alternatively activated or M2 (14, 16, 30). The deficiency of PAFR also resulted in weight gain, reduced glucose tolerance, increased expression of Ldlr in the liver and hepatocyte disarrangement, hepatic insulin resistance, and increased glucose levels. Under HFD, PAFR-deficient mice presented a severe insulin resistance that committed the liver and skeletal muscle compared to WT animals, followed by hepatic steatosis.

Both $CD11b^{+}Ly6C^{int}$ and $CD11b^{+}Ly6C^{high}$ mononuclear cells in the blood can be classified as pro-inflammatory monocytes and are likely to differentiate into M1 macrophages (28). We found that PAFRKO mice presented a higher population of $CD11b^{+}Ly6C^{high}$ cells, indicating that monocytes from these mice are already in a pro-inflammatory state. According to Ghanim et al. 2004, a pro-inflammatory state in peripheral blood mononuclear cells is associated with obesity and may contribute to insulin resistance (31). In fact, the adipose tissue macrophages from PAFRKO mice presented a pro-inflammatory M1 shifted phenotype. The macrophage switch to the pro-inflammatory profile is also linked to several metabolic diseases, including atherosclerosis (32), diabetic wound healing complications, and insulin resistance (5, 33). The fact that no difference in the expression of adiponectin and chemerin was found in adipose tissue indicates that the PAFR deficiency affects the inflammatory profile of macrophages rather than adipocytes. Moreover, it suggests that the knock down of PAFR induces a pro-inflammatory profile in monocytes that is maintained when they infiltrate into the adipose tissue and differentiate into macrophages.

Here we demonstrated that in SD, the pro-inflammatory monocytes/macrophages profile is correlated with an imbalance of glucose metabolism and insulin resistance in the liver, but not in the skeletal muscle. Since the insulin resistance occurs in the liver before the skeletal muscle (29), these results demonstrate that PAFR deficiency leads to susceptibility to the metabolic syndrome.

Liver steatosis is a hallmark of metabolic syndrome (6, 7) and PAFRKO mice presented increased liver weight and hepatocyte disarrangement already in SD. Confirming the susceptibility to develop hepatosteatosis, increased expression of the lipogenic gene Ldlr was found in the liver of PAFRKO mice in SD, and after HFD, these mice developed evident steatosis. Moreover, when fed HFD, PAFRKO mice presented a more prominent metabolic syndrome characterized by reduced glucose tolerance, increased insulin resistance, impairment of insulin signaling in both the liver and skeletal muscle.

HFD induces both insulin resistance and beta cell hyperplasia in human and mice model (34). Here, although mice fed HFD were insulin resistant (reduced insulin response in ITT and impaired insulin-induced AKT phosphorylation) the degree of resistance was not enough to affect the GTT. A possible explanation is that in response of a single dose of glucose used in GTT, hyperplasic beta cells would produce increased amount of insulin that compensate the insulin resistance during this test.Likewise is observed in patients in early stages of type 2-dyabetes(34).

We cannot exclude the possibility that PAFR deficiency directly affects adipocyte function rather than affecting the ATM. However, recent studies have demonstrated that the infiltration of pro-inflammatory macrophages into fat tissue is required in diet-induced insulin resistance (6-8, 10). Moreover, we found similar levels of adiponectin and chemerin, anti and pro-inflammatory adipokines respectively, suggesting that the ablation of PAFR does not affect the inflammatory profile in adipocytes. In brown adipose tissue, the PAFR activation was shown to up-regulate the expression of beta 3 adrenergic receptor and Uncoupling Protein 1, which are essential for cellular thermogenesis. These results suggest an additional mechanism where PAFR plays a role in metabolism by regulating energy expenditure (18). Addionally, studies in rats using Rupafin (Rupatadine), an antagonist of PAFR and H1 histamine receptors, showed microscopic liver findings in rats which comprised vacuolation of hepatocytes an increased incidence of fatty change (35). This strengthens our data, since we show possible mechanisms that might explain these side effects.

Using a different mouse strain (C57BL/6) to that employed in our study, Yamagushi*et al.*(17) demonstrated that the deficiency of PAFR exacerbated diet-induced glucose intolerance and no difference was found between WT and PAFKRO fed the SD. In our study, using the Balb/c background, we demonstrated that PAFRKO mice fed in SD were already glucose intolerant and hepatic insulin resistant, as observed by reduced insulin-induced AKT phosphorylation. Moreover, in our study using Balb/c mice, the glucose levels in SD-fed mice were higher in PAFRKO mice compared to WT, whereas similar levels of glucose were found in PAFRKO and WT mice of the C57BL/6 background (17). A possible explanation for these divergences is the difference in the mouse strain. Obese mice develop beta cell hypertrophy and hyperplasia, which can in part compensate the insulin resistance.In mice with a null mutation in the loci encoding the leptin receptor (*db/db* mice) or leptin (*ob/ob* mice), the C57BL/6 background was shown to be able to produce larger amounts of insulin compared to other mouse strains(36-38). Thus, it is possible that in C57BL/6 PAFRKO mice fed SD, the amounts of insulin produced during the glucose tolerance test is sufficient to control the glycemic levels, despite the insulin resistance. More studies comparing Balb/c and C57BL/6 mice regarding to glucose metabolism should be performed in order to unravel this hypothesis.

Insulin resistance is described as the failure of insulin to activate the PI3K/Akt pathway insulin receptor, which is closely associated with the dysregulation of glucose and lipid metabolism in the liver (39). Here, we observe that the PAFR deficiency led to

a decrease in Akt phosphorylation in the liver, an effect that is maximized in HFD. In previous publications, we showed that oxidized lipids induce Akt phosphorylation in macrophages in the absence of insulin and in a PAFR-dependent manner (40). PI3K/Akt pathway activation is associated with M2 macrophages polarization (41). Another possibility is that PAFR regulates hepatic glucose homeostasis via the Akt pathway; however, this hypothesis remains to be investigated.

A wide range of oxidized phospholipids that bind to PAFR are generated in the absence of enzymatic synthesis by various types of stressors. The mechanisms of generation of these oxidatively modified phospholipids and their effects were nicely reviewed by McIntyre in 2012 (13). The continuous removal of the oxidation products of these phospholipids is essential in aerobic organisms. Macrophages have the physiological function of removing oxidized molecules, altered cells and, during embryogenesis, tissues that are no longer required by the animal. This is achieved without causing inflammation, and has been known since the Metchnikoff Lectures in Comparative Pathology of Inflammation, 1892. Later on, a group of macrophage receptors was described to execute this function, named “scavenger receptors”, with CD36 being the prototypical receptor of this group. Our previous studies pointed to a central role for PAFR in this process. We found that CD36 co-localizes with PAFR in macrophage plasma membrane lipid rafts for optimal oxLDL uptake and apoptotic cells phagocytosis (14, 15). The association of these receptors shifted macrophages towards the anti-inflammatory phenotype. It can be speculated that this represents the “default” phenotype of macrophages since the scavenger function is a physiological event. Since PAFR is associated with this function, its activation by PAFR-ligands should maintain macrophages in an anti-inflammatory phenotype. We hypothesize that in the absence of PAFR, these oxidized moieties will bind to CD36, which would then interact with other receptors present in the membrane of macrophages, such as TLR4, 2, and 6 (42), shifting macrophages towards the classically activated phenotype. Although some of the molecular mechanisms are still elusive, this might explain some of the regulatory effects of PAFR found in our study. Thus, we postulate that, through PAFR, endogenously generated PAFR ligands maintain WAT macrophages in an anti-inflammatory profile. This process is essential to preserve adipose tissue homeostasis and balanced glucose metabolism.

Disclosures

No disclosures to declare.

Acknowledgments

This study was supported by the Fundação de Amparo à Pesquisa do Estado de São Paulo (FAPESP) and Conselho Nacional de Desenvolvimento Científico e Tecnológico (CNPq).

Author contribution statement

Study conception and design: Sonia Jancar and Francisco J. Rios

Acquisition of data: Luciano Ribeiro Filgueiras, Marianna Mainardi Koga, Paula G. Quaresma, Edson Kiyotaka Ishizuka, Marlise Montes and Francisco J. Rios

Analysis and interpretation of data: Luciano Ribeiro Filgueiras, Marianna Mainardi Koga, Paula G. Quaresma, Patricia O. Prada, Mario J. Saad, Sonia Jancar and Francisco J. Rios

Drafting of manuscript: Luciano Ribeiro Filgueiras, Sonia Jancar and Francisco J. Rios

Clinical perspectives

- In the obese stage, adipose tissue shows a high inflammatory profile accompanied by increased macrophage infiltration that leads to glucose intolerance and insulin resistance. Here, we investigated whether genetic deficiency of PAFR affects the phenotype of adipose tissue macrophages and its effect on glucose and insulin metabolism.
- Our results demonstrate that the absence of PAFR increases the inflammation in adipose tissue by leading macrophages towards M1 pro-inflammatory phenotype. Blood monocytes of PAFR KO mice also exhibit the pro-inflammatory phenotype. PAFR-ligands were detected in the serum of both, PAFR KO and WT mice. This results in metabolic disturbances, such as increase in weight gain, serum glucose, insulin resistance in the liver and skeletal muscle and severe liver damage, all hallmarks of metabolic syndrome.
- We identify a novel mechanism whereby PAFR activation regulates inflammation in adipose tissue and metabolic homeostasis.

References

1. Boyle JP, Thompson TJ, Gregg EW, Barker LE, Williamson DF. Projection of the year 2050 burden of diabetes in the US adult population: dynamic modeling of incidence, mortality, and prediabetes prevalence. Population health metrics. 2010;8:29.
2. Berrington de Gonzalez A, Hartge P, Cerhan JR, Flint AJ, Hannan L, MacInnis RJ, et al. Body-mass index and mortality among 1.46 million white adults. The New England journal of medicine. 2010;363(23):2211-9.
3. Westcott DJ, Delproposto JB, Geletka LM, Wang T, Singer K, Saltiel AR, et al. MGL1 promotes adipose tissue inflammation and insulin resistance by regulating 7/4hi monocytes in obesity. The Journal of experimental medicine. 2009;206(13):3143-56.
4. Nishimura S, Manabe I, Nagasaki M, Eto K, Yamashita H, Ohsugi M, et al. CD8+ effector T cells contribute to macrophage recruitment and adipose tissue inflammation in obesity. Nature medicine. 2009;15(8):914-20.
5. Wentworth JM, Naselli G, Brown WA, Doyle L, Phipson B, Smyth GK, et al. Pro-inflammatory CD11c+CD206+ adipose tissue macrophages are associated with insulin resistance in human obesity. Diabetes. 2010;59(7):1648-56.
6. Weisberg SP, McCann D, Desai M, Rosenbaum M, Leibel RL, Ferrante AW, Jr. Obesity is associated with macrophage accumulation in adipose tissue. The Journal of clinical investigation. 2003;112(12):1796-808.
7. Lumeng CN, Bodzin JL, Saltiel AR. Obesity induces a phenotypic switch in adipose tissue macrophage polarization. The Journal of clinical investigation. 2007;117(1):175-84.
8. Weisberg SP, Hunter D, Huber R, Lemieux J, Slaymaker S, Vaddi K, et al. CCR2 modulates inflammatory and metabolic effects of high-fat feeding. The Journal of clinical investigation. 2006;116(1):115-24.
9. Landmesser U, Cai H, Dikalov S, McCann L, Hwang J, Jo H, et al. Role of p47(phox) in vascular oxidative stress and hypertension caused by angiotensin II. Hypertension. 2002;40(4):511-5.
10. Spite M, Hellmann J, Tang Y, Mathis SP, Kosuri M, Bhatnagar A, et al. Deficiency of the leukotriene B4 receptor, BLT-1, protects against systemic insulin resistance in diet-induced obesity. Journal of immunology. 2011;187(4):1942-9.

11. Morris DL, Cho KW, Delproposto JL, Oatmen KE, Geletka LM, Martinez-Santibanez G, et al. Adipose tissue macrophages function as antigen-presenting cells and regulate adipose tissue CD4+ T cells in mice. Diabetes. 2013;62(8):2762-72.
12. Tamargo J, Tejerina T, Delgado C, Barrigon S. Electrophysiological effects of platelet-activating factor (PAF-acether) in guinea-pig papillary muscles. European journal of pharmacology. 1985;109(2):219-27.
13. McIntyre TM. Bioactive oxidatively truncated phospholipids in inflammation and apoptosis: formation, targets, and inactivation. Biochimica et biophysica acta. 2012;1818(10):2456-64.
14. Ferracini M, Rios FJ, Pecenin M, Jancar S. Clearance of apoptotic cells by macrophages induces regulatory phenotype and involves stimulation of CD36 and platelet-activating factor receptor. Mediators of inflammation. 2013;2013:950273.
15. Rios FJ, Ferracini M, Pecenin M, Koga MM, Wang Y, Ketelhuth DF, et al. Uptake of oxLDL and IL-10 production by macrophages requires PAFR and CD36 recruitment into the same lipid rafts. PloS one. 2013;8(10):e76893.
16. Mosser DM, Edwards JP. Exploring the full spectrum of macrophage activation. Nature reviews Immunology. 2008;8(12):958-69.
17. Yamaguchi M, Matsui M, Higa R, Yamazaki Y, Ikari A, Miyake M, et al. A platelet-activating factor (PAF) receptor deficiency exacerbates diet-induced obesity but PAF/PAF receptor signaling does not contribute to the development of obesity-induced chronic inflammation. Biochemical pharmacology. 2015;93(4):482-95.
18. Sugatani J, Sadamitsu S, Yamaguchi M, Yamazaki Y, Higa R, Hattori Y, et al. Antiobese function of platelet-activating factor: increased adiposity in platelet-activating factor receptor-deficient mice with age. FASEB journal : official publication of the Federation of American Societies for Experimental Biology. 2014;28(1):440-52.
19. Menezes-Garcia Z, Oliveira MC, Lima RL, Soriani FM, Cisalpino D, Botion LM, et al. Lack of platelet-activating factor receptor protects mice against diet-induced adipose inflammation and insulin-resistance despite fat pad expansion. Obesity. 2014;22(3):663-72.
20. Cecconello AL, Trapp M, Hoefel AL, Marques CV, Arbo BD, Osterkamp G, et al. Sex-related differences in the effects of high-fat diets on DHEA-treated rats. Endocrine. 2015;48(3):985-94.
21. Vasquez-Bravo YL, Russo M, Jancar S. Differential sensitivity of mouse strains to platelet activating factor-induced vasopermeability and mortality: effect of antagonists. Journal of lipid mediators. 1993;8(3):135-44.
22. Prada PO, Hirabara SM, de Souza CT, Schenka AA, Zecchin HG, Vassallo J, et al. L-glutamine supplementation induces insulin resistance in adipose tissue and improves insulin signalling in liver and muscle of rats with diet-induced obesity. Diabetologia. 2007;50(9):1949-59.
23. Ishii S, Nagase T, Shindou H, Takizawa H, Ouchi Y, Shimizu T. Platelet-activating factor receptor develops airway hyperresponsiveness independently of airway inflammation in a murine asthma model. Journal of immunology. 2004;172(11):7095-102.
24. Livak KJ, Schmittgen TD. Analysis of relative gene expression data using real-time quantitative PCR and the 2(-Delta Delta C(T)) Method. Methods. 2001;25(4):402-8.
25. Ferracini M, Sahu RP, Harrison KA, Waeiss RA, Murphy RC, Jancar S, et al. Topical photodynamic therapy induces systemic immunosuppression via generation of platelet-activating factor receptor ligands. The Journal of investigative dermatology. 2015;135(1):321-3.

26. Odegaard JI, Ricardo-Gonzalez RR, Goforth MH, Morel CR, Subramanian V, Mukundan L, et al. Macrophage-specific PPARgamma controls alternative activation and improves insulin resistance. Nature. 2007;447(7148):1116-20.
27. Kang K, Reilly SM, Karabacak V, Gangl MR, Fitzgerald K, Hatano B, et al. Adipocyte-derived Th2 cytokines and myeloid PPARdelta regulate macrophage polarization and insulin sensitivity. Cell metabolism. 2008;7(6):485-95.
28. Yang J, Zhang L, Yu C, Yang XF, Wang H. Monocyte and macrophage differentiation: circulation inflammatory monocyte as biomarker for inflammatory diseases. Biomarker research. 2014;2(1):1.
29. Kraegen EW, Clark PW, Jenkins AB, Daley EA, Chisholm DJ, Storlien LH. Development of muscle insulin resistance after liver insulin resistance in high-fat-fed rats. Diabetes. 1991;40(11):1397-403.
30. Filardy AA, Pires DR, Nunes MP, Takiya CM, Freire-de-Lima CG, Ribeiro-Gomes FL, et al. Proinflammatory clearance of apoptotic neutrophils induces an IL-12(low)IL-10(high) regulatory phenotype in macrophages. Journal of immunology. 2010;185(4):2044-50.
31. Ghanim H, Aljada A, Hofmeyer D, Syed T, Mohanty P, Dandona P. Circulating mononuclear cells in the obese are in a proinflammatory state. Circulation. 2004;110(12):1564-71.
32. Kanter JE, Kramer F, Barnhart S, Averill MM, Vivekanandan-Giri A, Vickery T, et al. Diabetes promotes an inflammatory macrophage phenotype and atherosclerosis through acyl-CoA synthetase 1. Proceedings of the National Academy of Sciences of the United States of America. 2012;109(12):E715-24.
33. Mirza RE, Fang MM, Weinheimer-Haus EM, Ennis WJ, Koh TJ. Sustained inflammasome activity in macrophages impairs wound healing in type 2 diabetic humans and mice. Diabetes. 2014;63(3):1103-14.
34. Golson ML, Misfeldt AA, Kopsombut UG, Petersen CP, Gannon M. High Fat Diet Regulation of beta-Cell Proliferation and beta-Cell Mass. The open endocrinology journal. 2010;4.
35. AusPAR. Rupafin Rupatadine iNova Pharmaceuticals. Australia 2011 [cited 2015 23/12]. 2011:[Available from: https://www.tga.gov.au/auspar/auspar-rupatadine.
36. Leiter EH, Coleman DL, Hummel KP. The influence of genetic background on the expression of mutations at the diabetes locus in the mouse. III. Effect of H-2 haplotype and sex. Diabetes. 1981;30(12):1029-34.
37. Filgueiras LR, Brandt SL, Wang S, Wang Z, Morris DL, Evans-Molina C, et al. Leukotriene B4-mediated sterile inflammation promotes susceptibility to sepsis in a mouse model of type 1 diabetes. Science signaling. 2015;8(361):ra10.
38. Coleman DL, Hummel KP. The influence of genetic background on the expression of the obese (Ob) gene in the mouse. Diabetologia. 1973;9(4):287-93.
39. Biddinger SB, Kahn CR. From mice to men: insights into the insulin resistance syndromes. Annual review of physiology. 2006;68:123-58.
40. Rios FJ, Koga MM, Ferracini M, Jancar S. Co-stimulation of PAFR and CD36 is required for oxLDL-induced human macrophages activation. PloS one. 2012;7(5):e36632.
41. Hyam SR, Lee IA, Gu W, Kim KA, Jeong JJ, Jang SE, et al. Arctigenin ameliorates inflammation in vitro and in vivo by inhibiting the PI3K/AKT pathway and polarizing M1 macrophages to M2-like macrophages. European journal of pharmacology. 2013;708(1-3):21-9.

42. Stewart CR, Stuart LM, Wilkinson K, van Gils JM, Deng J, Halle A, et al. CD36 ligands promote sterile inflammation through assembly of a Toll-like receptor 4 and 6 heterodimer. Nat Immunol. 2010;11(2):155-61.

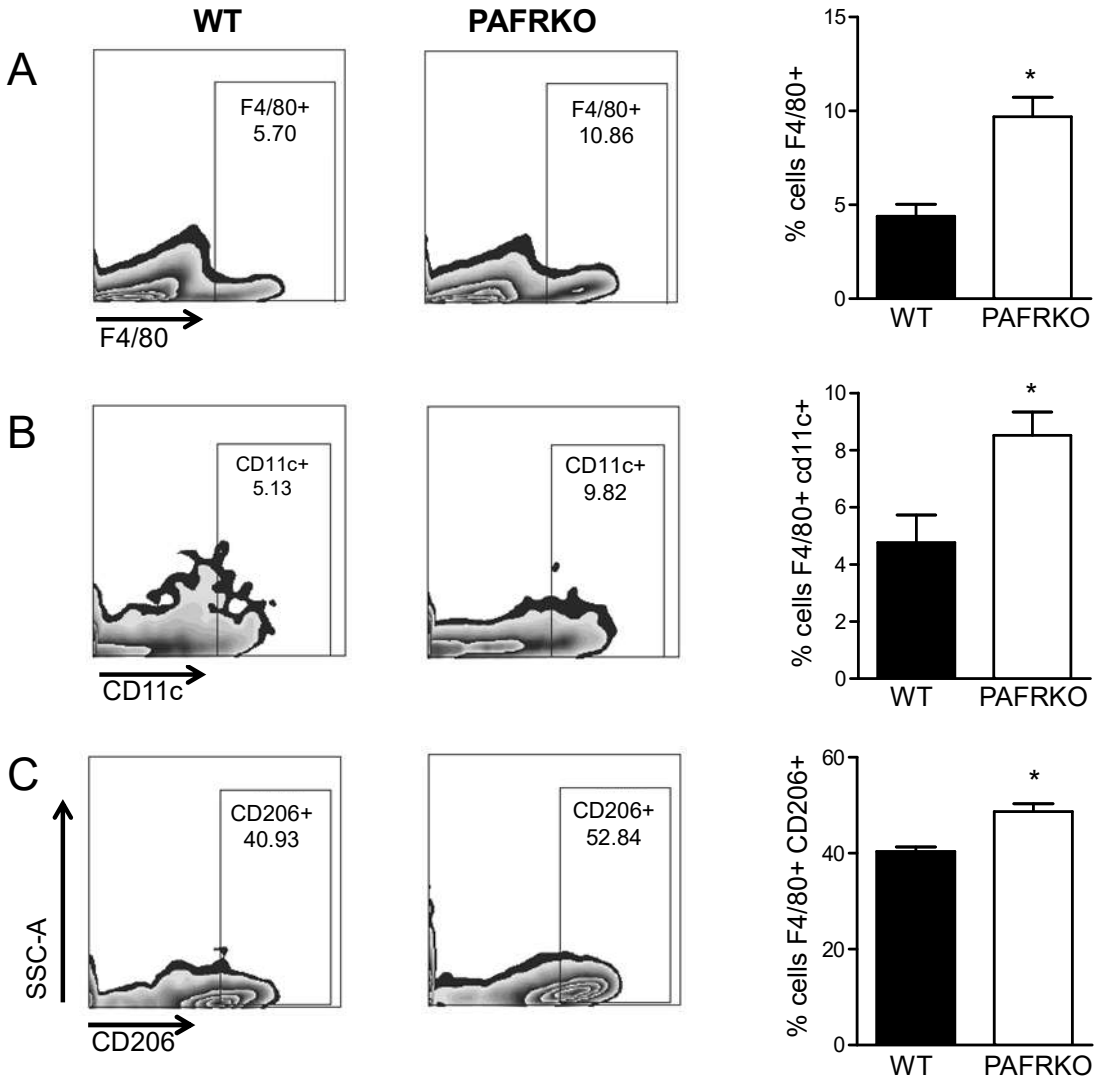

Figure 1: Deficiency of PAFR increases macrophage accumulation in adipose tissue. Epididymal adipose tissue macrophages from PAFRKO and WT mice were isolated by enzymatic digestion and stained for flow cytometry analysis. Results are shown as representative plots and as mean ± SEM of (A) $F4/80^+$ population (macrophages); (B) $CD11c^+$ population of $F4/80^+$ cells (M1 macrophages); (C) $CD206^+$

population of F4/80^{+} cells (M2 macrophages). (n=6-7) * p<0,05 PAFRKO *vs* WT animals.

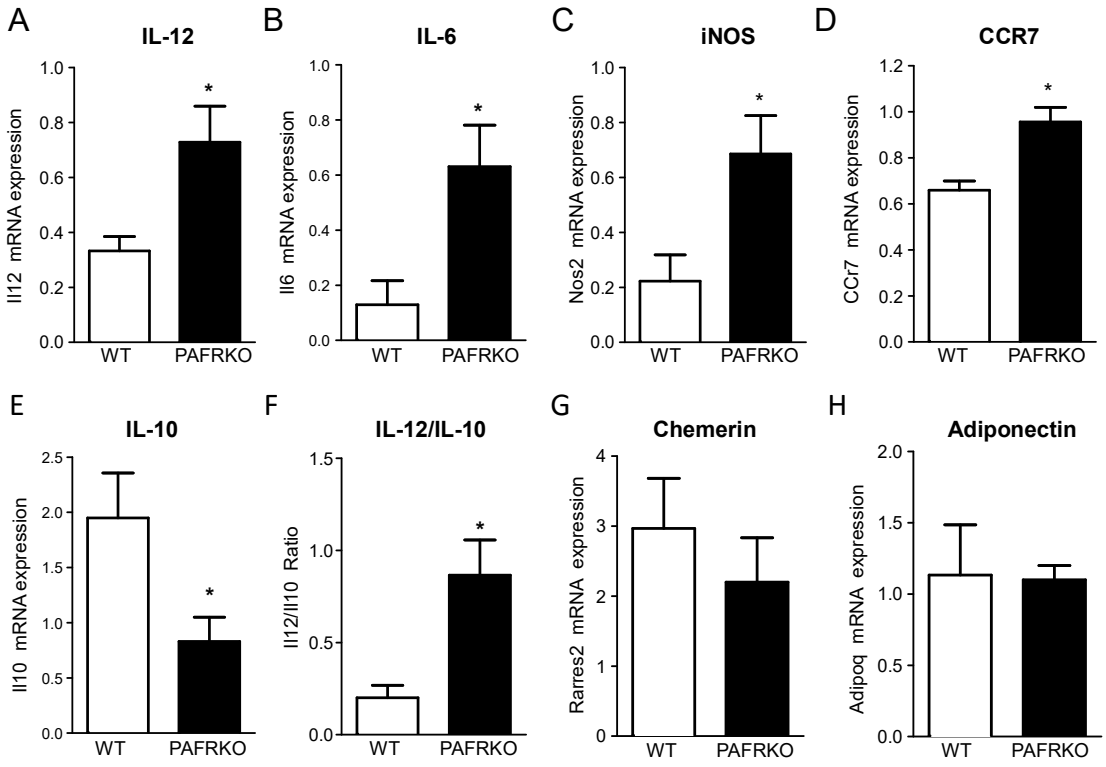

Figure 2: Adipose tissue from PAFR deficient mice show increased expression of pro-inflammatory markers. Total RNA was obtained from epididymal adipose tissue from PAFRKO and WT mice under SD. Macrophages markers (A-F) and adipokynes (G-H) gene expression was determined by RT-qPCR. Data are presented as mean ± SEM (n=6-7). *p<0.05 PAFRKO *vs* WT animals.

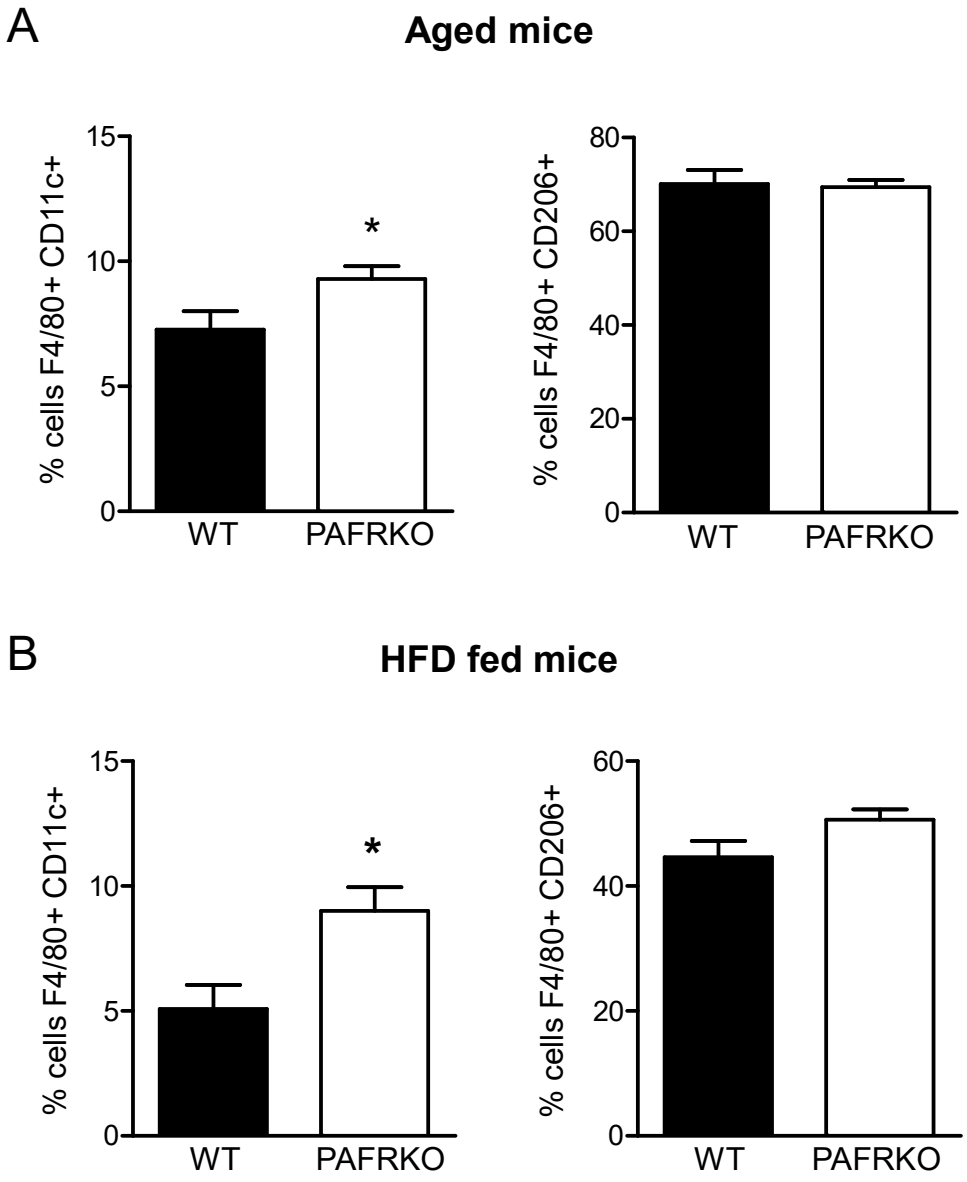

Figure 3: Advanced age and HFD increase M1 macrophages in adipose tissue of PAFR deficient mice. Epididymal adipose tissue macrophages from PAFRKO and WT mice were isolated by enzymatic digestion and stained for flow cytometry analysis. Results are shown as mean ± SEM of $CD11c^+$ population of $F4/80^+$ cells (M1 macrophages) and $CD206^+$ population of $F4/80^+$ cells (M2 macrophages) of (A) aged mice fed SD and (B) animals fed HFD. (n=6-7) *p<0,05 PAFRKO *vs* WT animals.

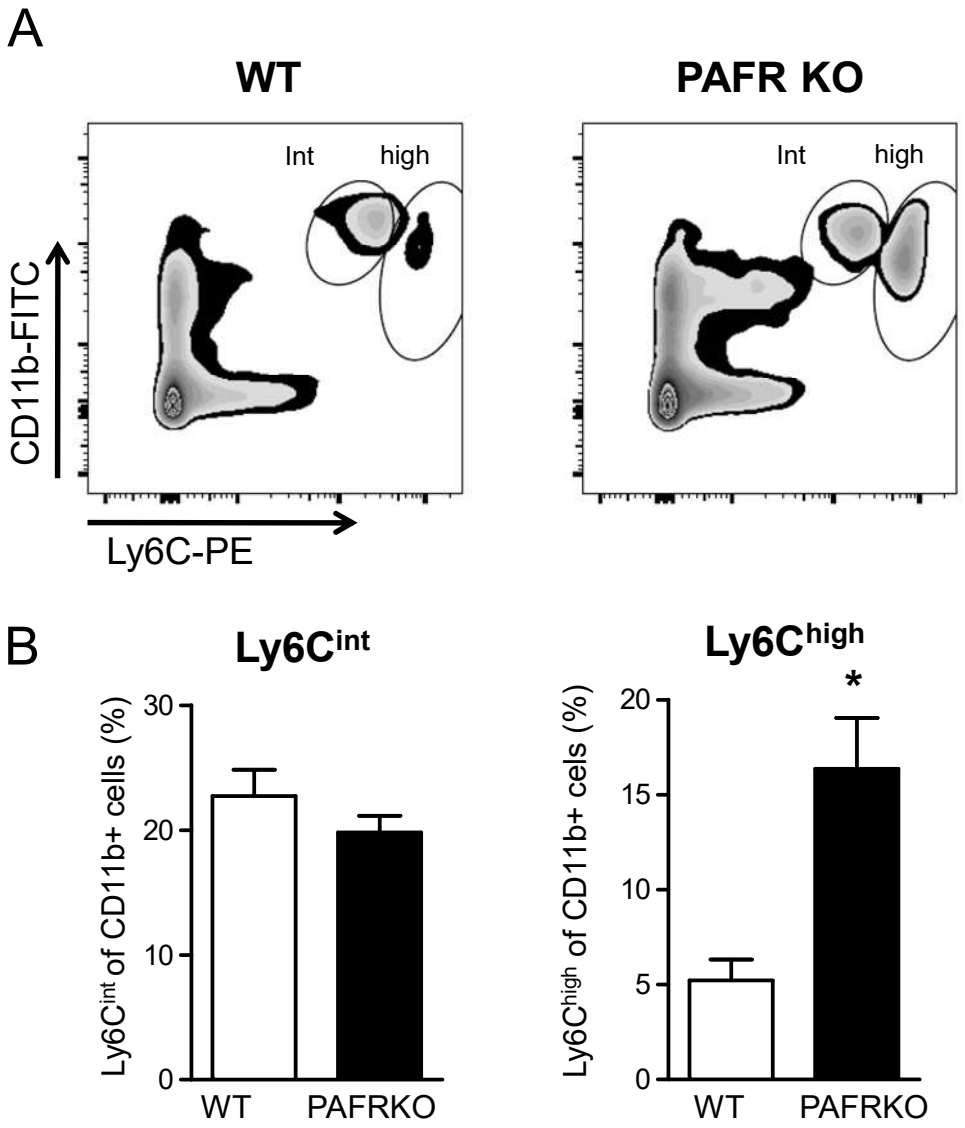

Figure 4 – PAFRKO mice have a higher percentage of pro-inflammatory monocytes in peripheral blood. PBMCs were isolated from blood of WT and PAFRKO mice and were stained for CD11b and Ly6C markers. Cells were gated as $CD11b^+$ and analyzed for $Ly6C^+$ cell population. **A**, representative plots of $CD11b^+Ly6C^+$ cells. **B**, percentage of $Ly6C^{int}$ and $Ly6C^{high}$ of $CD11b^+$ cells. * $P < 0.05$ (*n*=5).

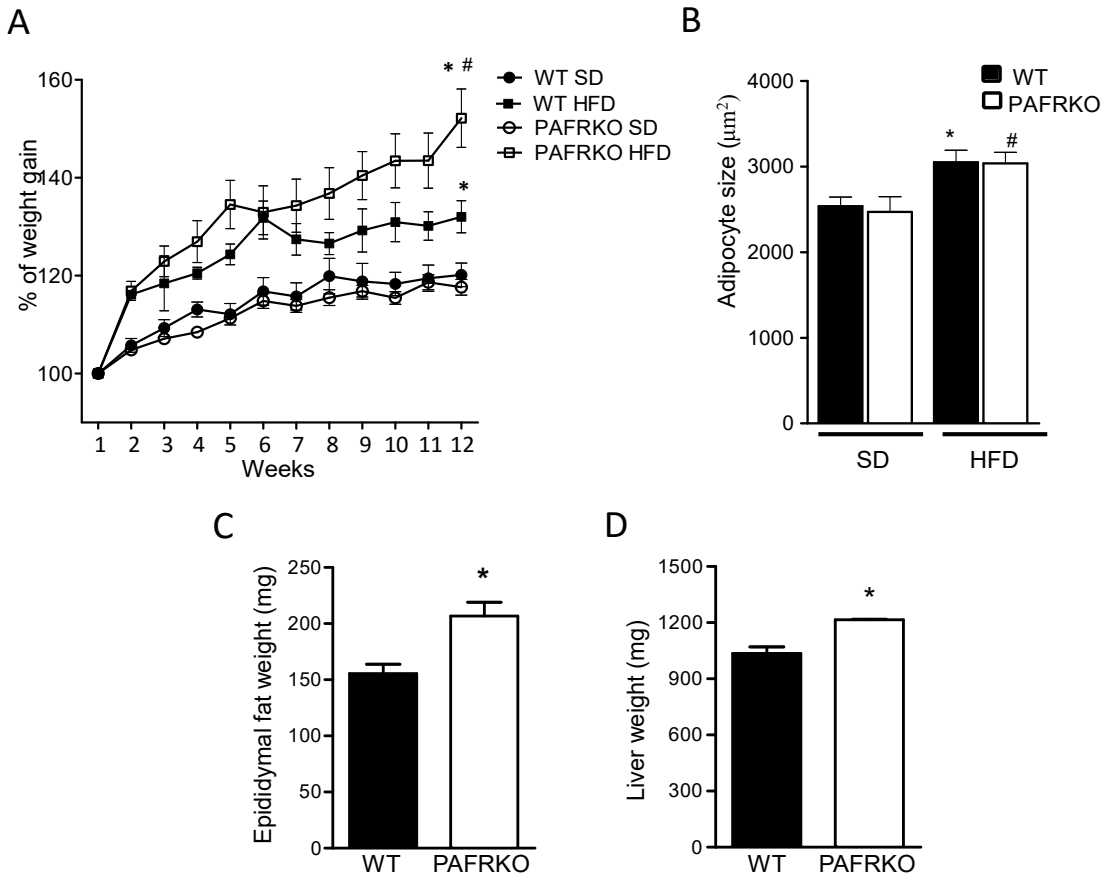

Figure 5: PAFR deficient mice gain more weight than WT. WT and PAFRKO mice were fed SD or HFD for 12 weeks and evaluated for weight gain (A), adipocyte size (B), weight of epididymal fat (C) and liver (D). Results are presented as percentage of weight gain or mg of weight. Adipocyte size was quantified in histologic sections from epididymal adipose tissue using ImageJ software and expressed as area ± SEM (n=7-9/group). *p<0.05 PAFRKO HFD *vs* PAFRKOSD or WT HFD *vs* WT SD and # p<0.05 PAFRKO HFD *vs* WT HFD.

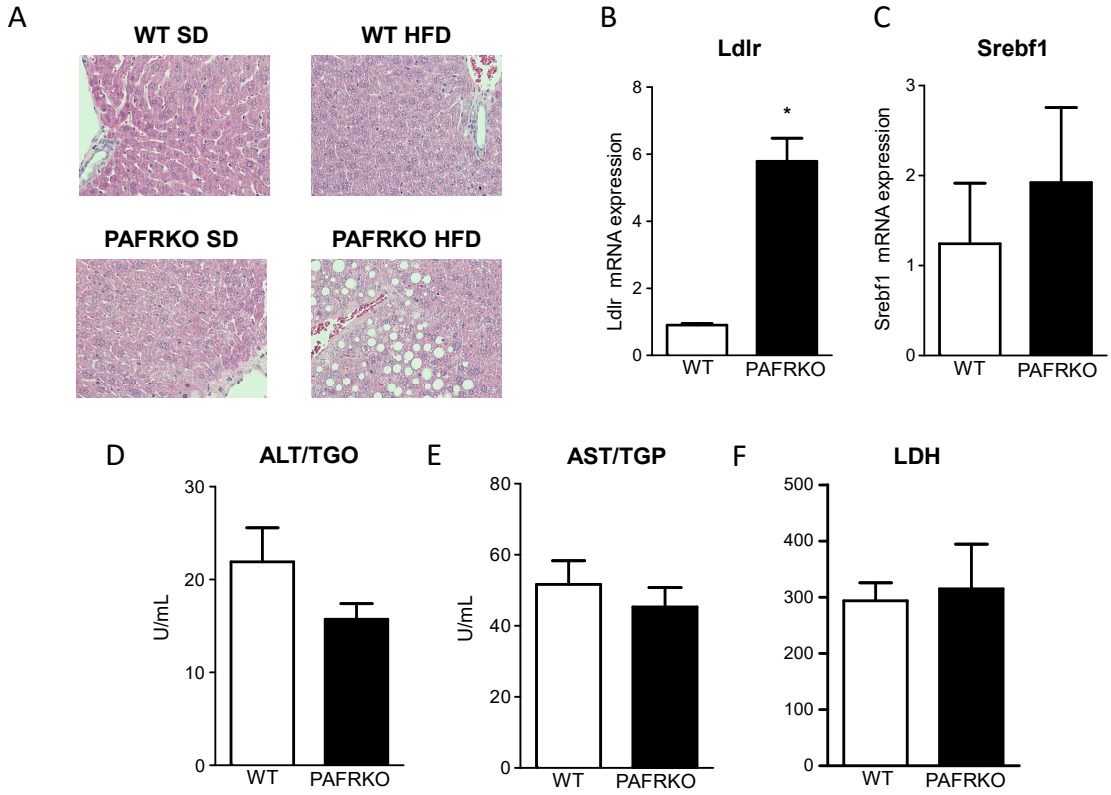

Figure 6: PAFR deficiency induces liver steatosis in mice fed HFD. Histological sections stained with HE were obtained from the liver of PAFRKO and WT mice fed SD and HFD for 12 weeks (A). Representative photomicrograph of 6-7 animals at 400 X magnification. Total RNA from the liver of PAFRKO and WT mice fed SD were obtained and Ldlr (B) and Srebf1 (C) gene expression was determined by RT-qPCR. Plasma was harvested from PAFRKO and WT mice fed SD and ALT/TGO (D), AST/TGP (E) and LDH (F) were determined. Data are presented as mean ± SEM (n=6-7). *p<0.05 PAFRKO *vs* WT animals

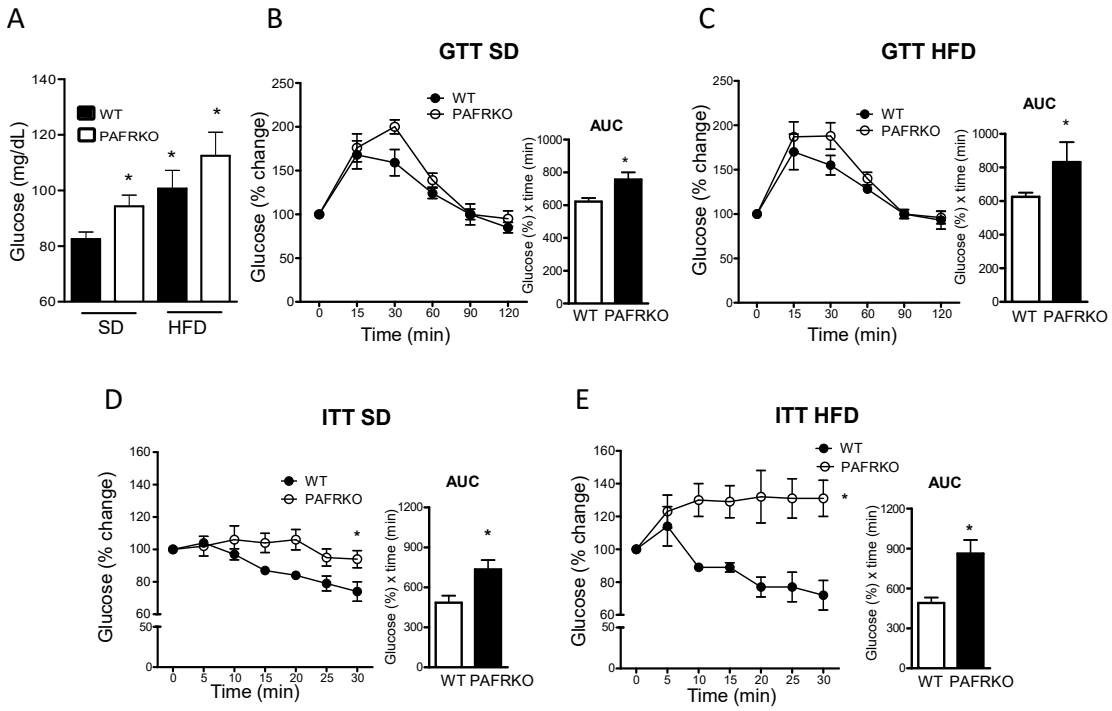

Figure 7: PAFR deficiency induces metabolic dysfunction. WT and PAFRKO mice were fed in SD or HFD. After 12 weeks animals were tested for fasting glucose (A), Glucose Tolerance Test (GTT) (B-C) and Insuline Tolerance Test (ITT) (D-E). Values are expressed in percentage and time zero was considered as 100%. Data are presented as mean ± SEM (n=7-9/group) *p<0.05 PAFRKO *vs* WT animals.

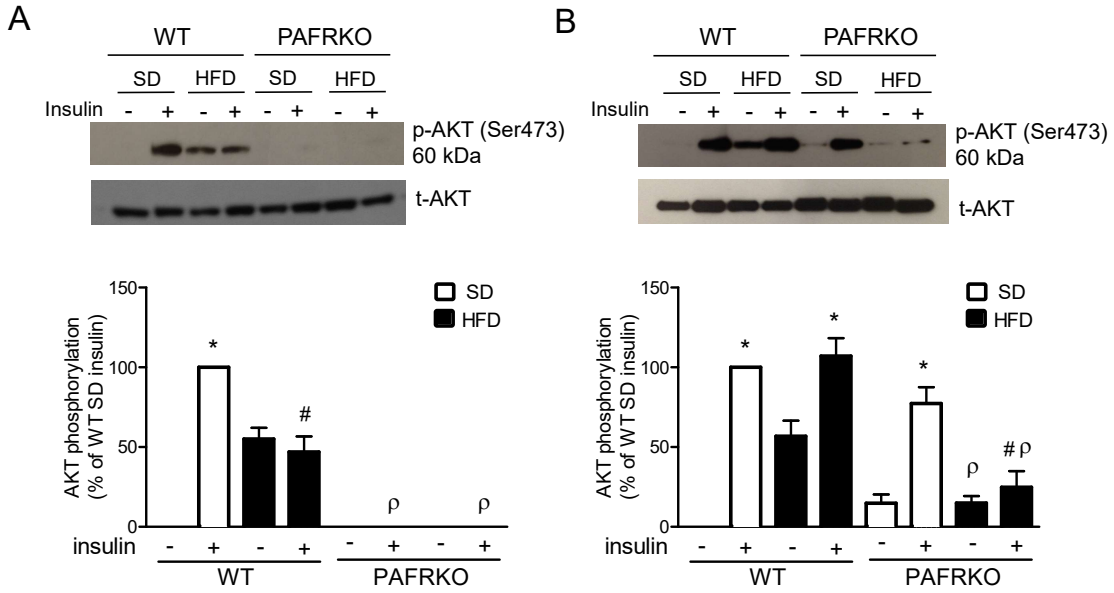

Figure 8: PAFR deficiency led to insulin resistance in liver and skeletal muscle and to hepatic steatosis. WT and PAFRKO mice were fed SD or HFD for 12 weeks. Five minutes after the insulin injection (3.8 U/kg i.p.), liver and skeletal muscle were removed. Phospho-Akt (p-Akt) was evaluated by western blot and normalized by total Akt in liver (A) and skeletal muscle (B). Data are shown as one representative experiment. Graph data are presented as mean ± SEM (n=4). *p<0.05 insulin treated *vs* non-treated, # p<0.05 HFD *vs* SD, and ρ p<0.05 PAFRKO *vs* WT. Histological sections were obtained from the liver and stained with HE (C). Representative photomicrograph of 6-7 animals at 400 X magnification.

PAFR in adipose tissue macrophages is associated with anti-inflammatory phenotype and metabolic homeostasis

Luciano Ribeiro Filgueiras[1], Marianna Mainardi Koga[1], Paula G. Quaresma[3], Edson Kiyotaka Ishizuka[1], Marlise B. A. Montes[1], Patricia O. Prada[3,4], Mario J. Saad[3], Sonia Jancar[1], and Francisco J. Rios [2]

[1]Department of Immunology, Institute of Biomedical Sciences, University of Sao Paulo, Sao Paulo, Brazil
[2]Institute of Cardiovascular and Medical Sciences, British Heart Foundation Glasgow Cardiovascular Research Centre, University of Glasgow, Glasgow, United Kingdom
[3]Department of Internal Medicine, State University of Campinas (UNICAMP), Campinas, SP, Brazil
[4]School of Applied Sciences, State University of Campinas (UNICAMP), Limeira, SP, Brazil.

Table S1. Sequences of mouse primers used for qPCR analysis

	Forward	Reverse
IL-12	5′-TGGTTTGCCATCGTTTTGCTG-3′	5′-ACAGGTGAGGTTCACTGTTTCT-3′
IL-10	5′-CAGAGCCACATGCTCCTAGA-3′	5′-TGTCCAGCTGGTCCTTTGTT-3′;
iNOS	5'-GTTCTCAGGCCAACAATACAAGA-3'	5'-GTGGACGGGTCGATGTCAC-3'
CCR7	5'-CAGGTGTGCTTCTGCCAAGAT-3'	5'-GGTATTCTCGCCGATGTAGTCA-3'
Chemerin	5'-CTAGGCCGGATAGTCCACTG-3'	5'-CCTGGAGAAGGCAAACTGTC-3'
Adiponectin	5'-TTGCAAGCTCTCCTGTTCCT-3'	5'-ATCCAACCTGCACAAGTTCC-3'
IL-6	5’- TCGGAGGCTTAATTACACATGTTC-3’	5’- TGCCATTGCACAACTCTTTTCT-3’
GAPDH	5′-AGGTCGGTGTGAACGGATTTG-3′	5′-TGTAGACCATGTAGTTGAGGTCA-3′

Supplemental Figure S1

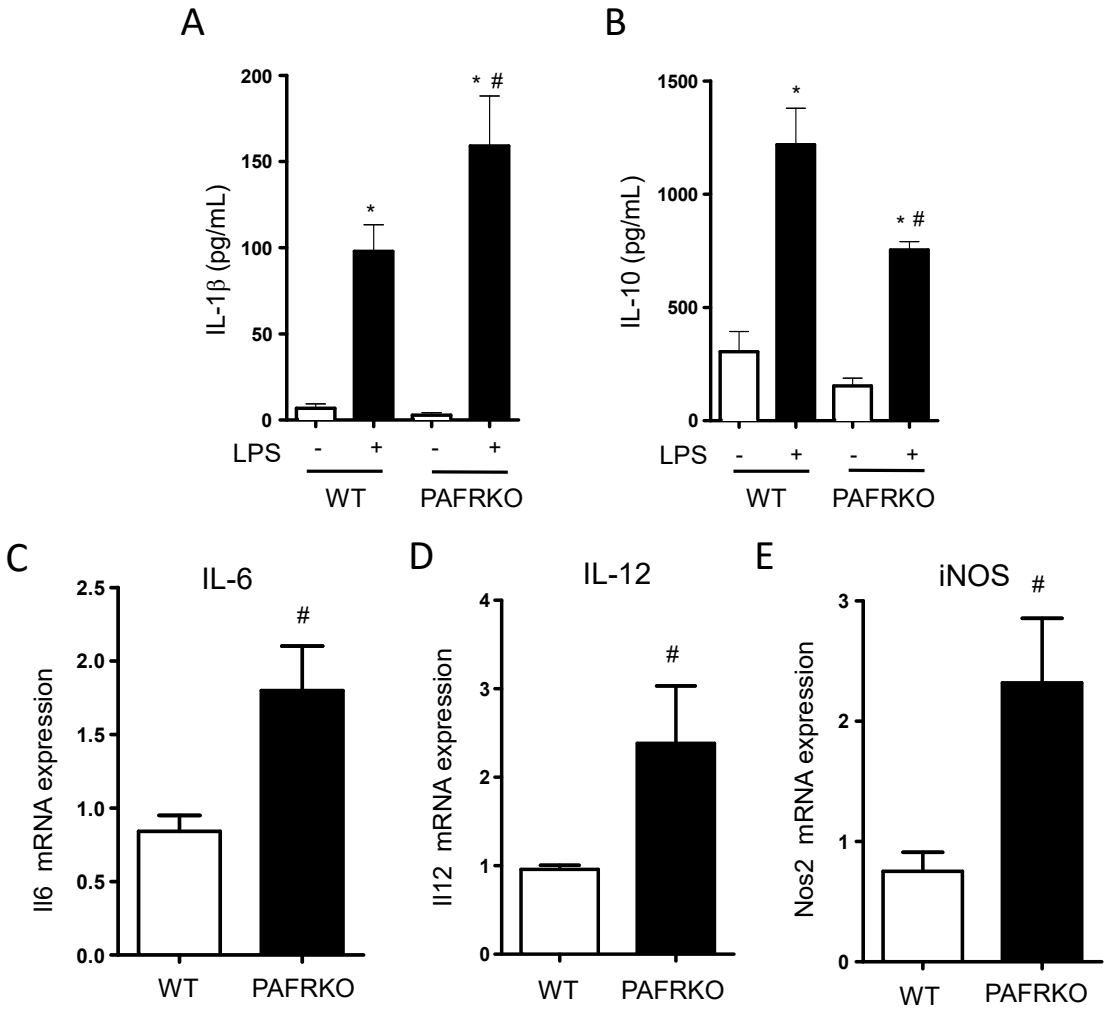

Supplemental Figure S1. PAFR deficient peritoneal macrophages present a pro-inflammatory phenotype. Resident peritoneal macrophages from WT and PAFRKO were obtained by peritoneal lavage and stimulated with LPS 100 ng/mL for 24 h. Concentrations of IL-1β (A) and IL-10 (B) in the supernatant were evaluated by ELISA. Total RNA from resident peritoneal macrophages of PAFRKO and WT mice, fed SD, were obtained and Il6 (C), Il12 (C) and Nos2 gene expression was determined by RT-qPCR.*$p<0.05$ PAFRKO or WT LPS stimulated *vs* non-stimulated and # $p<0.05$ LPS stimulated PAFRKO *vs* WT.

Supplemental Figure S2

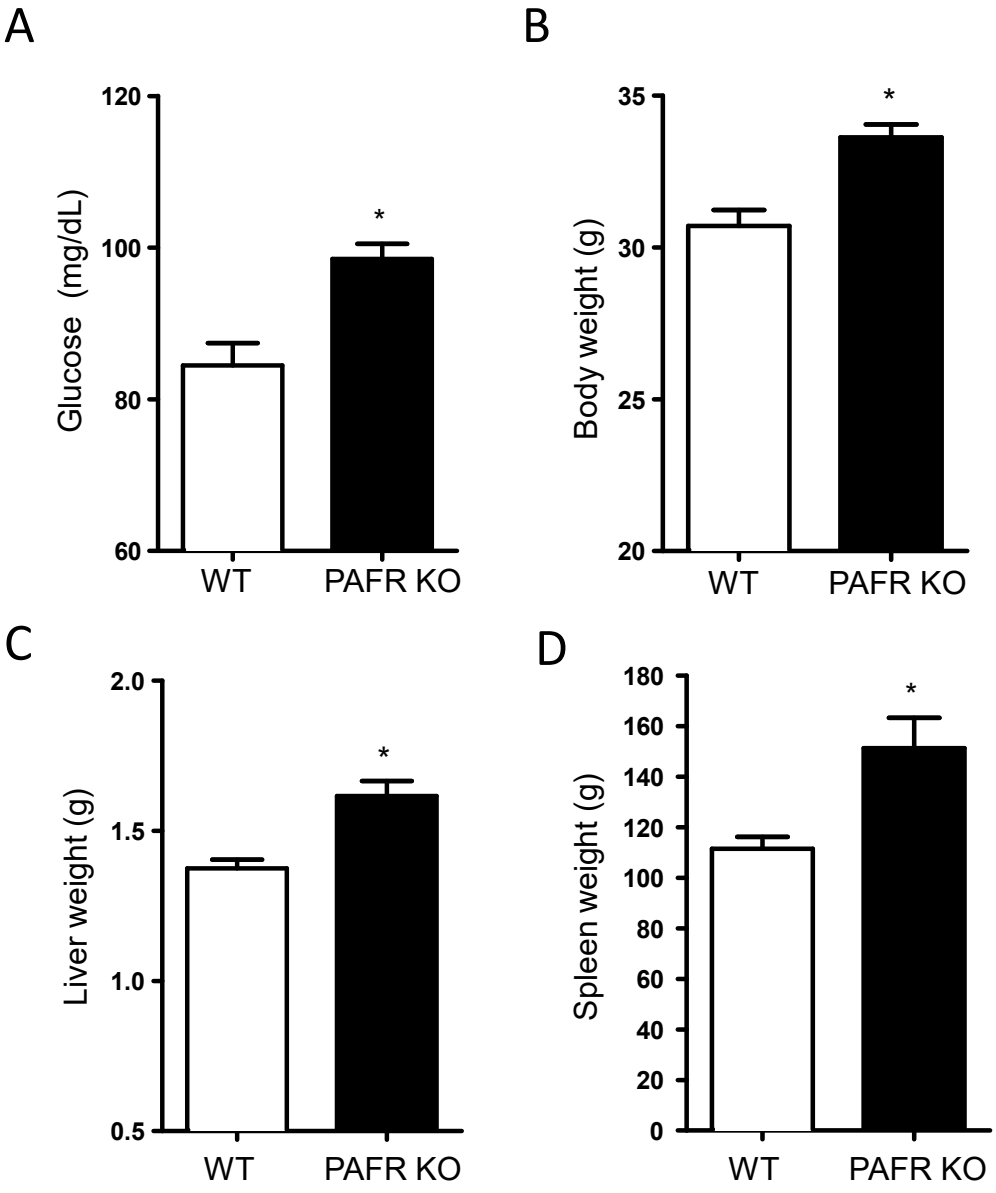

Supplemental Figure S2. Aged PAFR deficient mice present increased glucose level, body and liver weight. WT and PAFRKO mice were fed in standard diet for 40 weeks and analyzed for total fasting glucose levels (A), body (B), liver (C), and spleen (D) weight. Data are presented as mean ± SEM (n=5). *p<0.05 PAFRKO *vs* WT animals